

## The characterisation of ferroelectric thin films using nanoindentation

M. ALGUERÓ<sup>1</sup>, A.J. BUSHBY<sup>1</sup>, B.L. CHENG<sup>1</sup>, F. GUIU<sup>1</sup> AND M.J. REECE<sup>1</sup> M.L. CALZADA<sup>2</sup> AND L. PARDO<sup>2</sup>

<sup>1</sup>Department of Materials, Queen Mary and Westfield College, Mile End Road, E1 4NS, London, U.K.

<sup>2</sup>Instituto de Ciencia de Materiales, CSIC, Madrid 28049, Spain

Nanoindentation techniques have been used to determine the mechanical properties of two well characterised  $\text{Pb}_{0.88}\text{La}_{0.08}\text{TiO}_3$  ferroelectric thin films which have been shown to be promising for MEMs applications. A ceramic with the same nominal composition and the substrate material were also tested as an aid in the interpretation of results. Test routines have been developed using the spherical indentation geometry to distinguish the elastic and permanent deformation of the materials. Mechanical data for different layers in the heterostructure could be determined by using indenters with different radii. The technique provides information on the elastic modulus of the film, the onset and nature of permanent deformation, film delamination and the effects of porosity and residual stress. These techniques open the possibility to characterise fully the mechanical response of a microdevice.

*Keywords:* Ferroelectric thin films,  $\text{Pb}_{0.88}\text{La}_{0.08}\text{TiO}_3$ , nanoindentation, mechanical properties, MEMs.

### Caracterización de láminas delgadas ferroeléctricas por nanoindentación.

Se han usado técnicas de nanoindentación para determinar las propiedades mecánicas de dos láminas delgadas ferroeléctricas de  $\text{Pb}_{0.88}\text{La}_{0.08}\text{TiO}_3$  bien caracterizadas y que se han considerado prometedoras para aplicaciones MEMs. También se han realizado medidas en una cerámica con la misma composición nominal y en el sustrato de las láminas como ayuda para la interpretación de los resultados. Se han desarrollado rutinas usando la geometría de indentación con esfera para distinguir las deformaciones elástica y permanente del material. Podría ser posible obtener parámetros mecánicos de las distintas capas de la heteroestructura lámina sustrato mediante el uso de indentadores con radio distinto. La técnica proporciona información sobre el módulo elástico de la lámina, el comienzo y la naturaleza de la deformación permanente, delaminación y el efecto de la porosidad y las tensiones residuales. Estas técnicas abren la posibilidad de caracterizar completamente la respuesta mecánica de un microdispositivo.

*Palabras claves:* Láminas delgadas ferroeléctricas,  $\text{Pb}_{0.88}\text{La}_{0.08}\text{TiO}_3$ , nanoindentación, propiedades mecánicas, MEMs.

## 1. INTRODUCTION

Microelectromechanical systems (MEMs) are sensing and actuating devices in which the active element can be a ferroelectric thin film (1). The design of these devices requires reliable mechanical properties for the film, which is usually assumed to be the same as that of bulk ceramics (2,3). However, directly measured values for the Young's modulus of films are lacking. Although the development of MEMs involving ferroelectric films is in its early stages, their performance and reliability are becoming increasingly important. Elastic and permanent deformations induced during operation in the active and passive layers must be understood. Threshold stresses for ferroelastic domain reorientation in the film, which can lead to depolarisation phenomena, are also very important because they will determine the reproducibility of the performance and degradation of the device.

Nanoindentation is a powerful tool with high spatial resolution for mechanical characterisation of thin films (4,5). We present here results on the application of the technique to two well characterised  $\text{Pb}_{0.88}\text{La}_{0.08}\text{TiO}_3$  (PTL) ferroelectric thin films with different structure and microstructure, which have been shown to present good ferroelectric (6) and piezoelectric properties (7). A ceramic with the same nominal composition

and the substrate material were also tested to aid us in the discussion of the results. The technique is shown to be very useful for the study of the mechanical properties, not only of the film but also of the substrate underneath.

## 2. EXPERIMENTAL PROCEDURES

### 2.1. Materials

The two PTL ferroelectric films were prepared by a diol-based sol-gel technique. Both were single phase films with nominal composition  $\text{Pb}_{0.88}\text{La}_{0.08}\text{TiO}_3$  and the tetragonal perovskite structure. Films were prepared with 5 coatings of a precursor solution containing a 20 mole% excess of PbO on Pt/TiO<sub>2</sub>/Si-(100) substrates. The TiO<sub>2</sub> and Pt layers were 50 and 100 nm thick, respectively. The films were crystallised at 650°C with heating rates of either 10°C min<sup>-1</sup> or more than 500°C min<sup>-1</sup> in a conventional furnace, the latter rate being obtained by direct insertion after pre-heating. We will refer to them hereinafter as films of type A and B, respectively. More details on the preparation can be found elsewhere (8,9). Some

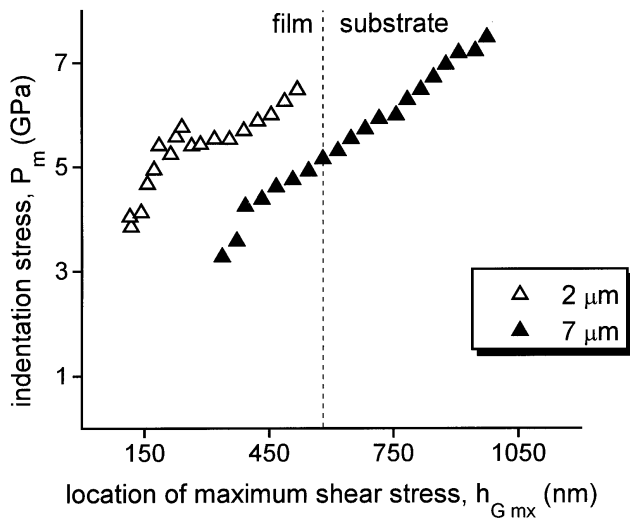


Figure 1. Location of the maximum shear stress as a function of the indentation stress for the PTL film type B with the two spherical indenter radii.

of the films structural and microstructural properties are listed in Table I. The values are taken from (6,7,9,10). An in plane tensile stress exists in both types of film, which is ~100 MPa higher in the type B film than in the type A film (11).

The ceramic with a nominal composition of  $Pb_{0.88}La_{0.08}(Ti_{0.98}Mn_{0.02})O_3$  was prepared by the conventional oxide mixing technique (12). Some of its structural and microstructural properties are also listed in Table I. No poling treatment was performed.

## 2.2. Mechanical characterisation

The mechanical behaviour of the materials was studied using a UMIS-2000 nanoindentation system. Two different spherical indenters with nominal radii of 2 and 7  $\mu m$  were used. By increasing the sphere radius, the location of the maximum shear stress,  $h_{G mx}$  for a given indentation stress,  $P_{m'}$  is shifted deeper into the thickness of the heterostructure (film plus substrate) under study. This allows the layer of the heterostructure to experience the highest stress to be selected, as it is illustrated for the PTL film type B in Figure 1, in which  $h_{G mx}$  is shown for different indentation stresses and for the two spherical indenters.

The basic measurement was a load,  $P$ , together with the sphere penetration into the heterostructure,  $h$ . Load cycles (loops) from zero to a given maximum load,  $P_{mx}$  and to zero again were recorded. The mechanical behaviour of a sample was obtained from the analysis of a set of consecutive loops at increasing maximum loads. One of these loops for the ceramic is shown in Figure 2a. The loop does not start at 0 penetration, but at a certain value, the remnant penetration,  $h_r$ , because of the plastic deformation produced by the previous indentation. The first parameter that it is extracted from each loop is the penetration at the maximum load,  $h_{p, mx}$  as shown in Figure 2a. The unloading part of the loop was then analysed as follows:

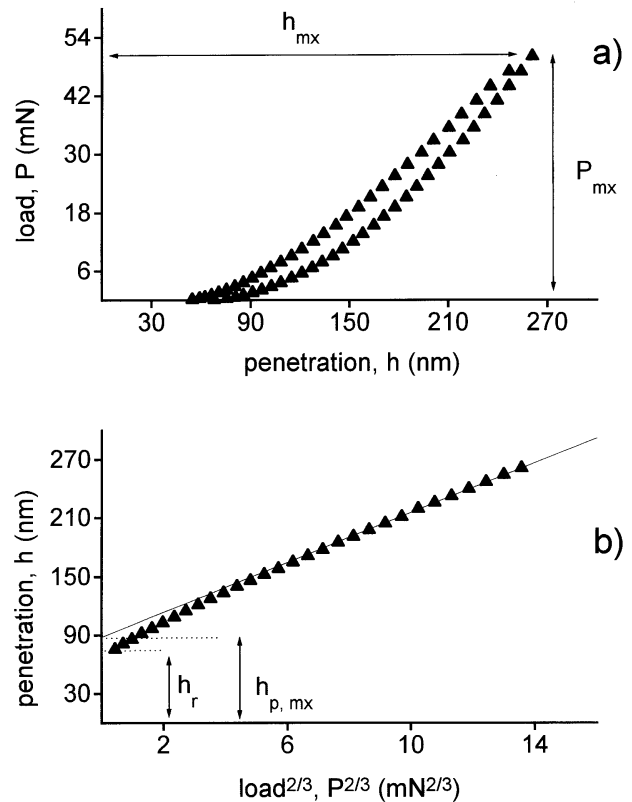


Figure 2. (a) A complete load penetration loop for the ceramic, and parameters extracted from it. (b) Unloading part of the previous loop, and parameters extracted from it.

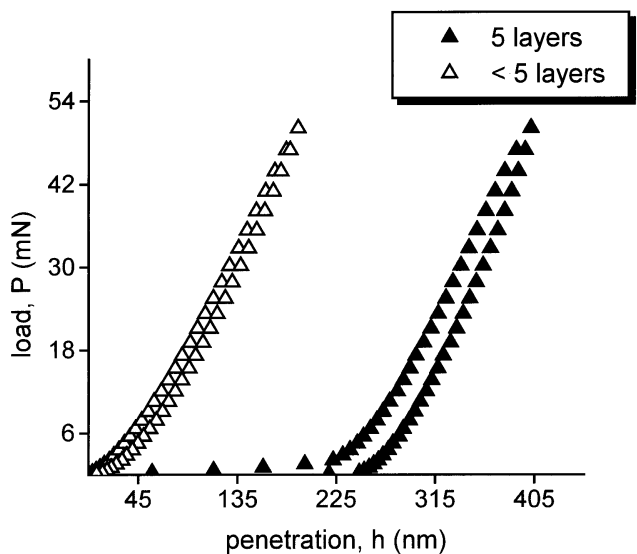


Figure 3. A typical load penetration loop for the film type A in an area with 5 coatings and in another with less than five coatings.

the penetration along the unloading step was plotted against  $P^{2/3}$ . This dependence is expected for a purely elastic indentation by a sphere and, therefore, the unloading is assumed to be elastic. This means that the permanent deformation is not reversed on unloading (13). The corresponding plot for the loop shown in Figure 2a is shown in Figure 2b. The linear fitting shown in Figure 2b was obtained with the first five points. The fitting is good up to 2/3 of the unloading, from where the experimental points deviate. This indicates that there was some recovery of the plastic deformation, or penetration relaxation, in the last part of the loop. By extrapolating the fitting to zero load,  $h_{p\_mx}$  is calculated, and from it, the depth of penetration in contact with the sphere (depth of contact),  $h_c$ , and the radius of the circle of contact,  $a$ , are obtained as explained in ref. 14. The latter magnitude allows to calculate the indentation stress,  $P_m$ , defined as the average pressure across the circle of contact, and the indentation strain,  $a/R$ , where  $R$  is the radius of the spherical indenter (15). The difference between  $h_{p\_mx}$  and the remnant penetration  $h_r$  is the relaxed penetration during unloading,  $h_{rx}$ . The slope of the fitting provides the Young's modulus of the sample.

### 3. RESULTS

The first observation was the presence of some delamination in the film type A. A typical loop for this film is shown in Figure 3, in which a penetration of  $\sim 200$  nm was observed as soon as the experiment began. The film coatings were not homogenous, and an area with less than five coatings existed, which did not show delamination. Results presented in this paper for this film correspond to the latter area. Changes of the film structure, microstructure and composition with the number of coatings are known to be not significant (6), therefore, large differences in the mechanical properties of films with different number of coatings are not expected.

The plastic penetration,  $h_{p\_mx}$  as a function of the indentation stress with the  $2 \mu\text{m}$  radius sphere is shown in Figure 4 for the different samples. The plastic penetration was negligible for

the substrate material as compared with the films or the ceramic. For the ceramic and the thin films, plastic deformation began during the first loop of the series (first point in Figure 4), and increased with the maximum load. Film type A showed considerable greater plastic deformation than either film type B or the ceramic.

The indentation stress-strain curves with the  $2 \mu\text{m}$  radius sphere are shown in Figure 5 for the different samples. The slope of the stress-strain curve was much lower for the film type A than for the film type B and the ceramic. The curve for both the film type B and the ceramic showed a change in slope or yield point at 5.6 and 5.4 GPa, respectively. This may indicate the onset of a new deformation mechanism, different to the one responsible for the deformation already occurring since the first loop (Figure 4). Stress-strain curves with the  $7 \mu\text{m}$  radius sphere are also shown for the two films in Figure 5. The strain for a given load for the film type A is significantly reduced, and the apparent yield point for the film type B disappeared.

Young's modulus,  $E$ , against the depth of contact with the  $2 \mu\text{m}$  radius sphere is shown in Figure 6 for the different samples. Film type B and the ceramic indicated an elastic modulus,  $E$ , of  $\sim 132$  GPa. For film type A the measured  $E$  was lower,  $\sim 102$  GPa. Elastic gradients were not observed, and the scattering at low depth of contact was most probably due to small deviations of the sphere radius from the nominal value. The Young's modulus with the  $7 \mu\text{m}$  radius sphere is also shown in Figure 6 for the two films. Values obtained are close to those of the substrate, 140 GPa.

### 4. DISCUSSION

Young's modulus results on the films with the two spheres clearly indicate that it is possible to obtain information from the different layers of the heterostructure by changing the radius of the sphere. Most of the indentation stress is applied to the ferroelectric film with the  $2 \mu\text{m}$  radius sphere. Therefore, the elastic response of the system is dominated by the respon-

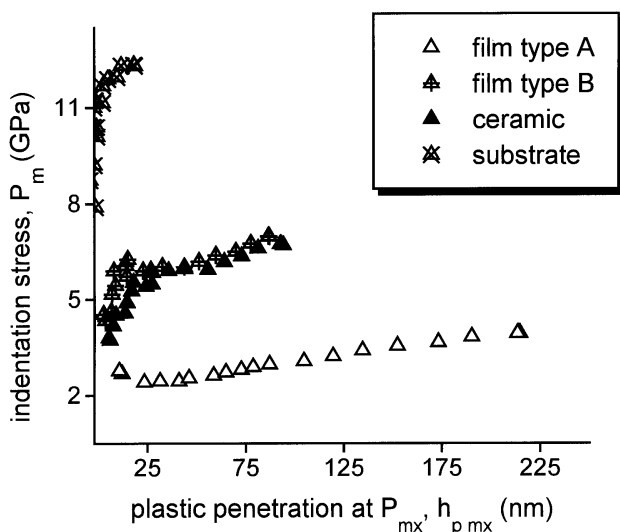


Figure 4. Plastic penetration as a function of the indentation stress with the  $2 \mu\text{m}$  radius sphere for the different PTL samples and the substrate.

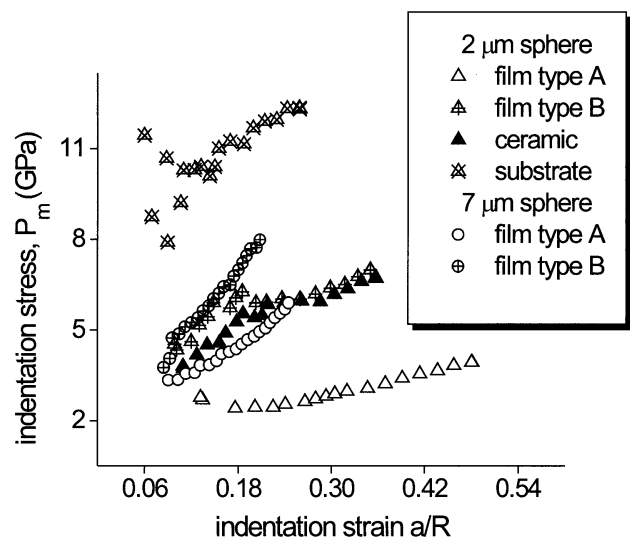


Figure 5. Indentation stress-strain curves for the different PTL samples and the substrate.

TABLE I. STRUCTURAL AND MICROSTRUCTURAL PROPERTIES OF THE DIFFERENT PTL SAMPLES

	perovskite orientation	tetragonal distortion	grain size ( $\mu\text{m}$ )	porosity (%)	pore size ( $\mu\text{m}$ )	thickness (nm)
film A	non oriented (9)	1.014 (9)	0.06-0.10 (10)	porous (9)	<0.05 (7)	645 (6)
film B	(001) (100) (9)	1.004 (9)	0.05-0.15 (10)	non porous (9)	-	560 (6)
ceramic	non oriented (12)	1.046 (12)	0.50 (12)	1.9% (12)	2.80 (12)	-

se of the film, and the obtained Young's modulus is that of the film (Figure 6). On the other hand, the maximum stress is shifted downwards with the 7  $\mu\text{m}$  radius sphere (Figure 1). Thus, the elastic response is then dominated by the substrate underneath, and its Young's modulus is obtained (Figure 6). The comparison of stress-strain curves with the two spheres (Figure 5) also allows to locate the layer in which a process is taking place. For instance, the large plastic deformation, as compared with other samples, occurring in film type A is really happening in the film and not in the substrate. The same occurs with the yield point in the stress-strain curve at 5.6 GPa in the film type B. Both features do not appear in the curve with the 7  $\mu\text{m}$  radius sphere. This ability to select the layer under study opens the possibility of study fully the mechanical response of MEM microdevices.

Plastic deformation in the ferroelectric samples was observed to begin during the first loop and to reach values as high as 213 nm in the film type A and  $\sim 90$  nm in the film type B and the ceramic (Figure 4). Such high values cannot be related to 90° domain reorientations but to another kind of mechanism. The fact that the process is much more significant in the film type A, which is known to be porous, suggests that it might be related to pore compaction (film densification). What might be related to domain reorientation is the apparent yield point observed in the ceramic and in the film type B at 5.4 and 5.6 Gpa, respectively. The higher value for the film could indicate some kind of domain clamping, most probably because of the

presence of the in plane tensile stress in the film. The effect of the stress could be much more significant than it looks like according to the small difference in the apparent yield point, because the yield point is higher in the film in spite of having a tetragonal distortion 0.042 smaller than the ceramic, as indicated in Table I. The stress at which the apparent yield point appears is very high as compared to the stresses reported to induce ferroelastic domain reorientation in ceramics (16). This could be because 5.4 GPa is an average pressure at the contact, and not the real value within the sample. Besides, it could be necessary to reach a threshold active volume (active means situation in which 90° domain reorientation occurs) to have a measurable effect. However, this is a subject for further research.

The film type A is not only special because of undergoing massive plastic deformation most probably through compaction, but because it presents a Young's modulus 23% lower than the one presented by the film type B and the ceramic (Figure 6). This is probably related also to the presence of pores. This fact illustrates perfectly how dangerous it could be to rely on parameters derived from bulk ceramics in the design of MEMs.

## 5. CONCLUSIONS

We have applied nanoindentation techniques using spherical indenters to study the mechanical behaviour of ferroelectric films. The properties of the film and the underlying substrate could be distinguished by selecting the radius of the spherical indenter, which is particularly relevant for MEMs. Porous PTL ferroelectric thin films showed massive permanent deformation at relatively low indentation stress, and a Young's modulus 23% lower than that of a ceramic with the same nominal composition. The behaviour of non porous films was very similar to that of the ceramic. Both showed a change in slope of the indentation stress-strain curve (yield point) at a specific indentation stress, which was higher for the film. This apparent yield point could be related to the onset of 90° domain reorientation, and the higher value for the film, to some clamping effect linked to the presence of the in plane residual stress in the film. These results have clear implications for the design and characterisation of MEMs.

## ACKNOWLEDGEMENTS

This work was funded through a Marie Curie Fellowship within the Training and Mobility of Researchers Programme of the European Commission (Contract n° ERBFMBICT983359), and through EPSRC Grant No GR/L90361.

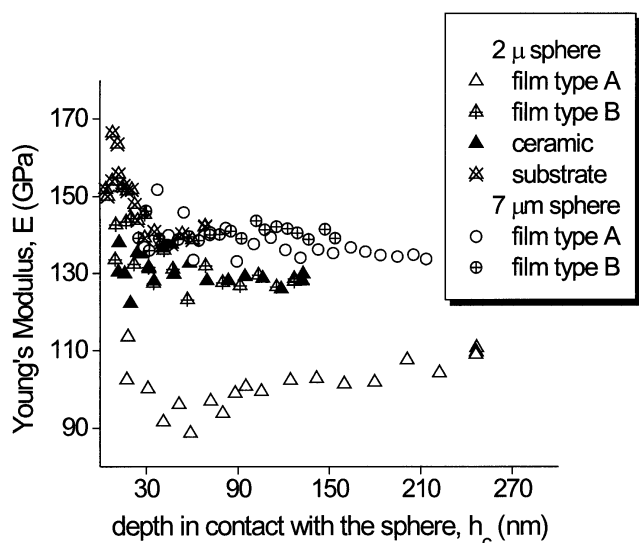


Figure 6. Young's modulus as a function of the depth of the contact for the different PTL samples and the substrate.

## REFERENCES

1. P. Muralt. "Piezoelectric thin films for MEMS". *Integrated Ferroelectrics* **17** 297-307 (1997).
2. D.F.L. Jenkins, M.J. Cunningham, G. Velu and D. Remiens. "High resolution micro-positioning of a silicon cantilever using sputtered PZT films". *Integrated Ferroelectrics* **17** 309-318 (1997).
3. G.A. Racine, P. Muralt and M.A. Dubois. "Flexural-standing-wave elastic force motor using ZnO and PZT thin film on micromachined silicon membranes for wristwatch applications". *Smart Mat. Struct.* **7** 404-416 (1998).
4. M.V. Swain and J. Mencik. "Mechanical property characterization of thin films using spherical tipped indenters". *Thin Solid Films* **253** 204-211 (1994).
5. A.J. Bushby and M.V. Swain. "Observation and analysis of a 200 nm aluminium film on silicon using ultra micro-indentation". In "Advances in Surface Engineering" 250-259. Eds. P.K. Datta and J.S. Burnell-Gray. Royal Society of Chemistry (1997).
6. M. Alguero, M.L. Calzada and L. Pardo. "The effect of film thickness on the ferroelectric properties of sol-gel prepared lanthanum modified lead titanate thin films". *J. European Ceramic Society* **19** 1481-1484 (1999).
7. M. Alguero. "Relaciones entre la microestructura y las propiedades de láminas delgadas ferroeléctricas de (Pb,La)TiO<sub>3</sub>". Tesis Doctoral. Universidad Autónoma de Madrid. Febrero 1998.
8. M.L. Calzada, M. Alguero and L. Pardo. "Chemistry crystallisation microstructure relations of sol-gel derived lanthanum modified lead titanate thin films". *J. Sol-Gel Sci. Tech.* **13**, 837-841 (1998).
9. M. Alguero, M.L. Calzada, C. Quintana and L. Pardo. "Ferroelectricity of lanthanum modified lead titanate thin films obtained by a diol based sol-gel method". *Appl. Phys. A* **68** 583-592 (1999).
10. M. Alguero, M.L. Calzada, E. Snoeck and L. Pardo. "Microstructure ferroelectric properties relationships in sol-gel prepared lanthanum modified lead titanate thin films". *J. European Ceram. Soc.* **19** 1501-1505 (1999).
11. M. Alguero, M.L. Calzada, L. Pardo and E. Snoeck. "On a combined effect of grain size and tensile stresses on the ferroelectric properties of sol-gel (Pb,La)TiO<sub>3</sub> thin films". Resubmitted to *J. Mater. Res.* After minor revision.
12. C.E. Millar, L. Pedersen, L. Pardo, J. Ricote, C. Alemany, B. Jiménez, G. Feuillard and F. Janin. "SAW properties of La, Sm modified lead titanate ceramics". *Proc. Electroceramics IV, Aachen (Germany) Sept. 5<sup>th</sup>-7<sup>th</sup> 1994*, **11** 1083-1088 (1994).
13. K.L. Johnson. "Contact mechanics". Cambridge University Press (1985).
14. J.S. Field and M.V. Swain. "Determining the mechanical properties of small volumes of material from submicrometer spherical indentations". *J. Mater. Res.* **10** 101-112 (1995).
15. A.J. Bushby. "Nano-indentation using spherical indenters". *Non Destructive Testing and Evaluation*. Accepted.
16. J.M. Calderón Moreno, F. Guiu, M. Meredith, M.J. Reece, N. McN. Alford and S.J. Penn. "Anisotropic and cyclic mechanical properties of piezoelectrics - compression testing". *J. European Ceram. Soc.* **19** 1321-1324 (1999).

